Published in final edited form as:
Eur J Neurosci. 2002 September ; 16(5): 795–806.

Connexin29 expression, immunocytochemistry and freeze-fracture replica immunogold labelling (FRIL) in sciatic nerve

Xinbo Li[1], **B. D. Lynn**[1], **C. Olson**[1], **C. Meier**[2], **K. G. V. Davidson**[3], **T. Yasumura**[3], **J. E. Rash**[3], and **J. I. Nagy**[1]

1 *Department of Physiology, Faculty of Medicine, University of Manitoba, 730 William Avenue, Winnipeg, Manitoba, Canada R3E 3J7*

2 *Department of Neuroanatomy and Molecular Brain Research, Ruhr-University Bochum, Universitaetsstrasse 150, D-44780 Bochum, Germany*

3 *Department of Anatomy and Neurobiology and Program in Molecular, Cellular and Integrative Neurosciences, Colorado State University, Fort Collins, CO 80523, USA*

Abstract

The recently discovered connexin29 (Cx29) was reported to be present in the central and peripheral nervous systems (CNS and PNS), and its mRNA was found in particular abundance in peripheral nerve. The expression and localization of Cx29 protein in sciatic nerve were investigated using an antibody against Cx29. The antibody recognized Cx29 in HeLa cells transfected with Cx29 cDNA, while nontransfected HeLa cells were devoid of Cx29. Immunoblotting of sciatic nerve homogenate revealed monomeric and possibly higher molecular weight forms of Cx29. These were distinguished from connexin32 (Cx32), which also is expressed in peripheral nerve. Double immunofluorescence labelling for Cx29 and Cx32 revealed only partial colocalization of the two connexins, with codistribution at intermittent, conical-shaped striations along nerve fibers. By freeze-fracture replica immunogold labelling (FRIL), Cx32 was found in gap junctions in the outermost layers of myelin, whereas Cx29-immunogold labelling was found only in the innermost layer of myelin in close association with hexagonally arranged intramembrane particle (IMP) 'rosettes' and gap junction-like clusters of IMPs. Although both Cx32 and Cx29 were detected in myelin of normal mice, only Cx29 was present in Schwann cell membranes in Cx32 knockout mice. The results confirm that Cx29 is a second connexin expressed in Schwann cells of sciatic nerve. In addition, Cx29 is present in distinctive IMP arrays in the inner most layer of myelin, adjacent to internodal axonal plasma membranes, where this connexin may have previously unrecognized functions.

Keywords

connexin29; connexin32; gap junctions; Schwann cells; sciatic nerve

Introduction

Connexins (Cx) form intercellular communicating channels for cell-to-cell exchange of ions and metabolites (Goodenough *et al.*, 1996; White & Bruzzone, 1996) and, in virtually all organs of the body, establish syncytial-like communities of gap junctionally coupled cells (Simon & Goodenough, 1998). The importance of gap junctional intercellular communication (GJIC) is supported by the lethality or physiological impairments caused by deletion of different connexin genes in mice, as well as by human diseases attributed to mutations in connexin genes

Correspondence: Dr J. I. Nagy, as above. E-mail: nagyji@ms.umanitoba.ca.

(Spray & Dermietzel, 1995; Willecke *et al.*, 2002). Diversity of GJIC is indicated by the existence of at least 20 genes coding for different, but homologous, connexin proteins; allowing for differential and regulated expression among diverse cell types. Complexity of GJIC is suggested by findings that cells frequently express two or more connexins within individual gap junction plaques (Severs, 1999; Rash *et al.*, 2001). Moreover, channels formed by different connexins display a broad range of gating properties and permeabilities (Veenstra, 1996). Many of the known connexins are expressed in the CNS. Of these, neurons express Cx36 (Condorelli *et al.*, 2000; Rash *et al.*, 2000, 2001), and astrocytes express Cx26, Cx30 and Cx43 (Nagy & Rash, 2000; Nagy *et al.*, 2001). Oligodendrocytes and Schwann cells previously were thought to express only Cx32 (Scherer *et al.*, 1995; Li *et al.*, 1997; Rash *et al.*, 2001), but recent reports have described Cx26, Cx43 and Cx46 in peripheral nerve (Yoshimura *et al.*, 1996; Chandross, 1998; Zhao & Spray, 1998; Mambetisaeva *et al.*, 1999), none of which has yet been localized to ultrastructurally identified gap junctions in PNS myelin.

The study of Cx32 in the PNS has intensified following the discovery that mutations in the Cx32 gene contribute to the human peripheral neuropathy Charcot-Marie-Tooth disease (CMTX) (Bergoffen *et al.*, 1993; Spray & Dermietzel, 1995; Bone *et al.*, 1997). Cx32 in peripheral nerves has been localized at Schwann cell nodes of Ranvier and at Schmidt-Lanterman incisures, which are conical-shaped cytoplasmic inclusions of noncompacted myelin (Bergoffen *et al.*, 1993; Scherer *et al.*, 1995) that contain a variety of proteins including myelin-associated glycoprotein (MAG), which has been shown ultrastructurally to be concentrated at, and is an accepted marker for, incisures (Trapp *et al.*, 1989; Arroyo & Scherer, 2000). Incisures may have specialized functions for metabolic and ionic communication (Ghabriel & Allt, 1981) mediated by gap junctions between the specialized myelin membranes that enclose successive cytoplasmic expansions (Balice-Gordon *et al.*, 1998). The Connexin29 (Cx29) gene has recently been cloned (Altevogt *et al.*, 2000; Sohl *et al.*, 2001), and its mRNA was shown to be expressed in adult mouse CNS, as well as in sciatic nerve where it was suggested to be expressed in Schwann cells (Sohl *et al.*, 2001). The presence of additional Schwann cell connexins and their functional relationship to Cx32 in peripheral nerve impacts on interpretations of the physiological basis of CMTX neuropathy. Consequently, an antibody against mouse Cx29 was used to begin analysis of the cellular and subcellular localization of Cx29 in the sciatic nerve.

Materials and methods

Antibodies and animals

An affinity-purified polyclonal antibody generated against a peptide corresponding to a sequence within the third cytoplasmic carboxy-terminus domain of Cx29 was obtained from Zymed Laboratories Inc (South San Francisco, CA, USA; Cat. no. 34–4200). Several anti-Cx32 antibodies with previously described specificities were used including sequence-specific 7C7, as well as 73F generated against full-length Cx32 (Li *et al.*, 1997). Antibodies 7C7 and 73F were kindly provided by E.L. Hertzberg (Albert Einstein College of Medicine, NY). Monoclonal antibody (Cat. No. MAB1567) against myelin-associated glycoprotein (MAG) was obtained from Chemicon International (Temecula, CA, USA). A total of 8 CD1 mice were obtained from the local Central Animal Care Services and utilized according to approved protocols by the Central Animal Care Committee, with minimization of stress to, and numbers of, animals used. Cx32 knockout-mice were kindly provided to one of us (J.E.R.) by K. Willecke (Bonn, Germany) and bred according to standard protocols. Tissues from six Cx32 knockout and six corresponding wild-type C57BL/6 were used in this study.

RT-PCR, Cx29 expression vector and immunoblotting

Total RNA was isolated from adult mouse brain and HeLa cells, and the reverse transcriptase reaction using 500 ng Oligo(dT)$_{15}$ Primer (Promega, Madison, WI, USA) was conducted as previously described (Lynn *et al.*, 2001). Oligonucleotide primers, materials for amplifying mouse Cx29 coding sequence and transfection reagents were purchased from Gibco BRL Life Technologies (Burlington, ON, Canada). Primers chosen for PCR were designed according to the mouse Cx29 sequence (Sohl *et al.*, 2001): sense primer, 5′-ATGTGCGGCAGGTTCCTGAGACA-3′; antisense primer, 5′-TCAAAATGGCTCTTTTGCCTCCA-3′. PCR was carried out in 20 μL of solution containing 2 μL of 10 X PCR buffer (Gibco BRL), 0.8 μL of 50 mM $MgCl_2$, 200 μM dNTP, 100 ng sense and antisense primers, 1 unit of Taq DNA polymerase and 1 μL of template cDNA. PCR products were separated by electrophoresis in a 1% agarose gel, stained with ethidium bromide and purified using a gel purification kit (Qiagen Inc, Mississauga, ON, Canada). pcDNA3 vector with CMV promoter was obtained from Invitrogen (Burlington, Ont, CA) and pcDNA3-T vector was prepared according to standard protocol. PCR products were ligated into pcDNA3-T vector using T4 DNA ligase (Promega). Recombinant plasmids were extracted, orientation was verified with BamHI digestion, and at least two recombinant plasmids were sequenced (ABI-320 DNA sequencer) using T7 universal primer for confirmation of sequence. HeLa cells (American Type Culture Collection, Rockville, MD, USA) were grown in Dulbecco's Modified Eagle's medium (DMEM) supplemented with 10% fetal bovine serum and 1% penicillin-streptomycin, and maintained in an incubator at 37°C with 5% CO_2. Cells were transiently transfected with plasmid using Lipofect AMINE 2000 (Gibco BRL Life Technologies) reagent and taken for analysis 48 h post-transfection.

Mice were killed by decapitation, and samples of sciatic nerve and liver were homogenized in RIPA buffer (50 mM Tris-HCl, pH 8.0, 10 mM $MgCl_2$, 150 mM NaCl, 1% Triton-X 100, 1 mM phenyl-methylsulphonylfluoride (PMSF) and 2 μg/mL each of pepstatin A and leupeptin). HeLa cells were rinsed with cold 10 mM sodium phosphate buffer, pH 7.4, containing 0.9% saline (PBS) and harvested in RIPA buffer. Homogenates were sonicated, proteins were separated on 12.5% sodium dodecylsulphate polyacrylamide gel electrophoresis (SDS-PAGE) (30 μg per lane, samples not boiled prior to loading), transblotted to 0.2 μm polyvinyl difluoride (PVDF) and probed with antibodies as previously described (Li *et al.*, 1997; Nagy *et al.*, 2001) using anti-Cx29 (2 μg/mL) or anti-Cx32 antibody 73F (from mouse acities fluid; diluted 1 : 1000) or 7C7 (from unconcentrated culture supernatant; diluted 1 : 25). For analysis of specificity by peptide preadsorption, 1 μg of anti-Cx29 was preincubated for 1 h at room temperature with or without 100 μg of immunizing peptide and then incubated with blots or tissues.

Immunohistochemistry

Mice were deeply anaesthetized and perfused transcardially with fixative, and tissues were dissected and stored in cryoprotectant (Li *et al.*, 1997). Cryostat sections (10 μm) collected on gelatinized glass slides were processed by immunofluorescence labelling for Cx29 and/ or Cx32. Antibody dilutions and incubations were performed in buffer containing 1.5% NaCl, 50 mM Tris-HCl, pH 7.6, 0.3% Triton X-100 and 4% normal donkey serum (TBST). For single labelling, sections were incubated for 24 h at 4°C with either polyclonal anti-Cx29 (2 μg/mL) or with monoclonal mouse anti-Cx32 (73F diluted 1 : 1000 or 7C7 diluted 1 : 50). Sections were washed for 1 h in TBST and then incubated for 1.5 h at room temperature with either Cy3-conjugated donkey anti-rabbit IgG (Jackson ImmunoResearch Laboratories, West Grove, PA, USA) diluted 1 : 200 for polyclonal Cx29, or Cy3-conjugated goat anti-mouse IgG (Jackson ImmunoResearch Laboratories) diluted 1 : 200 for monoclonal Cx32 antibodies. Cultures of HeLa cells were rinsed with cold PBS, fixed in ice-cold 0.1 M sodium phosphate buffer, pH 7.4, containing 4% formaldehyde, and processed with anti-Cx29 as above. Double

immunofluorescence labelling was performed by simultaneous incubation of anti-Cx29 with either anti-Cx32 (73F, diluted 1 : 1000), anti-Cx32 (7C7, diluted 1 : 50) or anti-MAG (diluted to 2 μg/mL) followed by simultaneous incubation with Cy3-anti-rabbit IgG and fluorescein isothiocyanate (FITC)-conjugated horse anti-mouse IgG (Vector Laboratories) diluted 1 : 50. Fluorescence was examined on a Zeiss Axioskop2 MOT fluorescence microscope equipped with filters for visualization of FITC (excitation, 450–490 nm; emission 515–550 nm) and Cy3 (excitation, 541–551 nm; emission, 565–595 nm), and on an Olympus Fluoview IX70 confocal microscope. Images were captured using Zeiss AxioVision 3.0 or Fluoview software, assembled according to appropriate size and adjusted for contrast based on elimination of 'empty' pixels in either Photoshop version 3.0 or Corel Draw version 8.

Freeze-fracture replica immunogold labelling

Normal and Cx32 knockout mice were anaesthetized with ketamine/ xylazine (90 mg/kg and 8 mg/kg) and fixed by transcardiac perfusion with 2% formaldehyde. Sections of sciatic nerve were frozen, freeze-fractured in a JEOL/RMC RFD 9010C freeze-fracture device, and prepared for FRIL as previously described (Rash & Yasumura, 1999; Rash *et al.*, 2001). Replicas were single- or double labelled with rabbit anti-Cx29 antibodies (listed above) and monoclonal antibodies to Cx32 (Zymed Laboratories Inc, Chemicon International Inc, Temecula, CA, USA). Secondary immunogold-labelling was with various combinations of goat anti-mouse and goat anti-rabbit IgG bound to 5-nm (BBInternational, Cardiff, UK) and 6-nm, 12- and/or 18-nm gold (Jackson ImmunoResearch Laboratories). In some experiments, the use of two or more sizes classes of immunogold beads to label each connexin facilitated detection of gap junctions in low magnification searches based on higher visibility of the larger gold beads, yet retained the higher labelling efficiency of the smaller gold beads (Nagy *et al.*, 2002). In addition, the simultaneous presence of two sizes of gold beads in each of two different structures (i.e. gap junctions vs. rosettes) and absence of the other sizes of gold beads in the same structure provides an internal verification of labelling specificity for each primary antibody. In these replicas, 'signal-to-noise' ratios (defined in Rash & Yasumura, 1999) were 500 : 1–5000 : 1.

Replicas were photographed as stereoscopic pairs in a JEOL 2000 EX-II TEM (included angle of 8E) at initial magnifications from 5 000 × to 100 000 ×. One sample labelled with 5- and 6-nm gold is presented in reverse stereo perspective ('intaglio'), which clearly reveals that these small, low contrast gold beads are not coplanar with or part of the platinum replica film. As an aid to interpreting image details, stereoscopic images should be viewed using a 2× magnification, parallel optical axis (Stereopticon-type) viewer. Images were prepared with Photoshop 6.01, using minimal unsharp mask, levels and selected area dodging (brightness and contrast) functions to optimize image contrast and definition.

Results

Cx29 antibody characterization

In homogenates of sciatic nerve, affinity-purified anti-Cx29 antibody detected three major bands at approximately 32, 52 and 74 kDa (Fig. 1A, lane 1). The monomeric form of Cx29 migrated slightly slower than its predicted molecular weight. Bands at 52 and 74 kDa may represent nondissociated dimeric and trimeric forms of Cx29, but this remains to be established. Such aberrant migration profiles of monomeric and multimeric forms of other connexins have been reported (Green *et al.*, 1988;Matesic *et al.*, 1993;Rash *et al.*, 2000). However, we cannot exclude that these band arise from cross-reactions of antibody with other proteins on immunoblots. For comparison, homogenates of liver probed with anti-Cx32 antibody contained monomeric Cx32 at 30 kDa, as well as higher molecular weight forms (Fig. 1A, lane 2). Cx29 antibody did not detect Cx32 when used to probe immunoblots of liver homogenate

(Fig. 1A, lane 3). Based on the different migration profiles of Cx29 and Cx32, the anti-Cx29 and anti-Cx32 antibodies do not cross-react with Cx32 or Cx29, respectively. In a separate blot of sciatic nerve homogenate, the bands detected by anti-Cx29 (Fig. 1B, lane 1) were eliminated after preadsorption of antibody with immunizing peptide (Fig. 1B, lane 2).

In two separate experiments, Western blots of lysates from communication-deficient HeLa cells transiently transfected with Cx29 cDNA revealed detection of monomeric Cx29 (Fig. 2A, lanes 2 and 3) with a migration profile similar to that of Cx29 in homogenates of sciatic nerve (Fig. 2A, lane 1). Lysates from HeLa cells transfected with empty vector showed an absence of the monomeric Cx29 immunoreactive band (Fig. 2A, lane 4). Higher molecular weight bands detected by Cx29 antibody in empty vector-treated cells obscured detection of Cx29 dimeric forms in Cx29 cDNA transfected cells. As a further control, RNA extracted from cells transfected with Cx29 cDNA and empty vector was taken for RT-PCR using Cx29 primers, and analysis by agarose gel electrophoresis indicated the presence of PCR products of expected size in the former, but not in the latter (not shown). Immunofluorescence labelling with anti-Cx29 antibody in transfected HeLa cells is shown in Fig. 2B. A small percentage of cells in cultures transfected with Cx29 expression vector displayed bright immunofluorescence, while cultures treated with empty vector were devoid of labelling (Fig. 2C). Although some proportion of immunoreactivity appeared to be localized intracellularly, labelling was particularly evident around the periphery of cells (Fig. 2B, inset).

Immunofluorescence for Cx29 and Cx32 in sciatic nerve

Optimal immunofluorescence labelling for Cx29 was achieved by perfusion with 4% formaldehyde/picric acid fixative with either no postfix or 1.5 h postfix. A low magnification view of Cx29 immunofluorescence in a 1-mm segment of sciatic nerve is shown in Fig. 3A. Individual fibers exhibit cross striations of intermittent labelling. As shown in Fig. 3B and C, the striations often had a conical appearance. Also seen were narrow bands of labelling orientated perpendicular to the length of fibers. Examination of these by through focus indicated that most of these were also conical in shape, but their narrowed portions were only weakly labelled or were out of the plane of focus. More rarely encountered were abutments of concentrated immunofluorescence on each side of what were likely nodes of Ranvier (Fig. 3C). Laser scanning confocal microscopy indicated that conical immunolabelling associated with fibers was arranged as circular collars outside the margins of axons and that no labelling was seen within axons (Fig. 3D and E). Confocal microscopy also confirmed dense labelling at nodes of Ranvier (Fig. 3F), although it was difficult to discern the organization of Cx29 distribution at these structures.

Sections of sciatic nerve were processed for simultaneous labelling of Cx29 and Cx32 using two different anti-Cx32 antibodies. Double immunofluorescence indicated that most Cx29-immunoreactive cross striations along fibers (Fig. 4A) were also labelled for Cx32 with monoclonal anti-Cx32 antibody 73F (Fig. 4B). Similar results were obtained when sections were labelled for Cx29 (Fig. 4C) and simultaneously with monoclonal antibody 7C7 (Fig. 4D). Double-labelling for Cx29 (Fig. 4E) and MAG (Fig. 4F) also indicated a high degree of colocalization of these two proteins, indicating Cx29 localization at Schmidt-Lanterman incisures. In control procedures, omission of one or the other of the primary antibodies with inclusion of both of the secondary antibodies produced no inappropriate labelling (i.e. Cy3 labelling with rabbit primary or FITC labelling with monoclonal primary), indicating lack of cross reactions of the secondary antibodies used.

Adjacent sections of nerve processed for immunohistochemistry by standard procedures using Cx29 antibody or antibody that had been preadsorbed with immunizing peptide are shown in Fig. 5. The robust labelling observed with anti-Cx29 (Fig. 5A) was eliminated after antibody preadsorption (Fig. 5B). In order to establish lack of immunohistochemical cross reaction of

anti-Cx29 antibody with Cx32, sections of liver were processed for Cx29/Cx32 double-labelling concurrently with sciatic nerve as above. Anti-Cx32 antibodies gave a typical pattern of punctate labelling around hepatocytes (Fig. 5C), while anti-Cx29 antibody produced no labelling (Fig. 5D).

To establish lack of immunohistochemical detection of Cx29 by the anti-Cx32 antibodies utilized, sections of sciatic nerve from Cx32 knockout mice were processed for Cx29/Cx32 double-labelling. In the Cx32 knockout C57BL/6 strain of mice, labelling for Cx29 (Fig. 6A) was similar to that observed in both wild-type C57BL/6 mice (not shown) and CD1 mice (Fig. 3), but was not examined in detail for possible quantitative differences. A total absence of labelling was seen in sections of nerve from knockout mice processed with anti-Cx32 antibody 73F (Fig. 6B) or with 7C7 (not shown), which is in contrast to the normal pattern of immunolabelling seen with these antibodies in sections of sciatic nerve from wild-type strain C57BL/6 mice (Fig. 6C). These results indicate lack of anti-Cx32 antibody cross-reaction with Cx29. Also evident in the absence of Cx32 labelling in the KO mice (Fig. 6B) is the level of background seen in sciatic nerve with the antibodies employed as well as the pattern of background, which is distinctly different than the specific labelling.

FRIL localization of Cx29 and Cx32

Replicas of normal sciatic nerve that were single- and double-labelled for Cx32 and/or Cx29 revealed distinctive distributions for each connexin. Cx32 was found in conventional ‘plaque-type’ gap junctions within internodal myelin (Fig. 7). A detailed description of the distributions of Cx32 in gap junctions of normal vs. Cx32 KO mice is in preparation (C. Meier, R. Dermietzel, T. Yasumura and J. E. Rash, unpublished observations). As in homologueous gap junctions in all other tissues examined by FRIL (e.g. Rash *et al.*, 2001), Cx32 immunogold labelling was equally common beneath both E- and P-face gap junction plaques. In contrast, immunogold labelling for Cx32 could not be detected in Cx32 KO mice in gap junctions of liver or of sciatic nerve (not shown).

Cx29 immunogold labelling was abundant in the innermost layer of myelin in both normal mice (Fig. 8A and B) and in Cx32 KO mice (Figs 8C and 9), where it was detected only in association with unusual ‘rosettes’ of hexagonally arranged 8-nm P-face IMPs, clusters of hexagonally and randomly arranged 8-nm IMPs, and with singlet and doublet 8-nm IMPs. Unlike Cx32, Cx29 was not detected in gap junctions in the outer layers of myelin, in Schmidt-Lanterman incisures, or linking successive loops of paranodal myelin. However, in paranodal loops directly abutting the axon plasma membrane, immunogold labelling also was found on rosettes, interlocking rosettes and clusters of IMPs (Fig. 9C). Significantly, Cx29 immunogold labelling was not detected beneath myelin E-faces, nor did a search for labelling result in detection of rings or clusters of E-face pits. This apparent restriction of labelling to P-face IMPs and lack of labelling of myelin E-faces is noteworthy because E- and P-faces are produced in equal numbers (Challcroft & Bullivant, 1970; Steere, 1971), and E- and P-faces are equally well labelled in homologous gap junctions (e.g. astrocyte-to-astrocyte, or neuron-to-neuron) but are not labelled equally at heterologous gap junctions containing different connexins on each side of the junction (e.g. oligodendrocyte-to-astrocyte gap junctions) (Rash *et al.*, 2001). Thus, the asymmetry of labelling of P-faces *vs.* E-faces in the innermost layer of myelin may provide an important clue regarding the nature of the coupling partner, if any, for Cx29.

Discussion

We used a newly generated antibody against Cx29 to demonstrate the expression and localization of Cx29 protein in peripheral nerve. Antibody specificity was established by several methods including Cx29 recognition in HeLa cells transfected with Cx29 expression vector. In view of the coexpression of Cx29 and Cx32 in nerve fibers, care was taken to establish

that Cx29 antibody does not cross-react with Cx32 and that Cx32 antibody does not cross-react with Cx29. In addition, specificity of Cx32 detection is indicated by the presence of Cx32 immunofluorescence or immunogold labelling in gap junctions in mouse liver and myelin in normal mice, but not in liver or myelin of Cx32 KO mice. Finally, Cx29 but not Cx32 immunogold labelling of rosettes and clusters of 8-nm IMPs in the innermost layer of myelin in sciatic nerve of normal and Cx32 KO mice and lack of Cx29 labelling at sites in normal myelin where Cx32 was found further indicates that anti-Cx29 recognizes Cx29 but not Cx32.

Cx29 and Cx32 coexpression

Earlier observations raised the possibility that, in addition to their expression of Cx32, Schwann cells may contain additional connexins. Single channel analyses indicated that coupling of Schwann cell pairs is mediated by gap junction channels having several discrete conductances, suggesting the presence of more than one connexin (Chandross, 1998). Further, injection of low molecular weight dyes into the outer cytoplasmic collar of Schwann cells resulted in radial dye-transport along pathways of uncompacted myelin towards the inner cytoplasmic collar, and this radial pathway was suggested to consist of gap junction channels composed of Cx32 at Schmidt-Lanterman incisures (Balice-Gordon *et al.*, 1998). Based on findings that radial dye-transport in nerves of Cx32 knockout mice was largely unimpaired, Balice-Gordon *et al.* 1998 suggested that other Schwann cell connexins may be able to form channels at incisures in the absence of Cx32. Support for these observations may be provided by the finding of Cx29 as a second connexin in Schwann cells (Sohl *et al.*, 2001), by demonstration of high Cx29 mRNA expression in peripheral nerve (Sohl *et al.*, 2001), by the present LM results showing Cx29 colocalization with Cx32 and MAG in nerve, and by the continued expression of Cx29 in sciatic nerve of Cx32 KO mice.

However, interpretation of the degree to which Cx29 compensates for deletion of Cx32 requires caution. First, loss of Cx32 in mice and Cx32 mutations in humans do, after all, result in peripheral neuropathies. Second, radial dye-transport in nerves of Cx32-deficient mice may appear largely normal due to a partial contribution of Cx29 or another connexin, combined with possibly abnormally enhanced transport through structurally abnormal myelin (Suter, 1995; Anzini *et al.*, 1997; Sahenk & Chen, 1998) including enlarged Schmidt-Lanterman incisures. Third, Cx29 was found by FRIL in IMP rosettes and clusters in the innermost layer of myelin in both normal and Cx32 KO mice, but did not occur at sites in the outermost layer of myelin, where Cx32 is found in normal mice. Fourth, while radial dye transport in nerves is inferred to be mediated by junctions at incisures and at paranodal loops, the presence of gap junctions at these locations remains to be established.

Ultrastructural localization

Cx32 has not been localized by immunoultrastructural methods at Schmidt-Lanterman incisures or at paranodal loops in CNS or PNS. Therefore, it is important to note that the occurrence of gap junctions at these structures has been inferred solely from its colocalization with other proteins know to be concentrated in incisures of peripheral nerve (Scherer, 1996). Considering our LM observations, we in turn infer Cx29 to be targeted to incisures and paranodal loops based on its colocalization with MAG and its partial codistribution with Cx32. However, while it is true that gap junctions have been observed between successive paranodal loops in mammalian CNS (Sandri, 1977; J. E. Rash, unpublished observations), and rare gap junctions have been reported to link the outer layers of myelin in normal avian PNS and to increase dramatically during Wallerian degeneration (Tetzlaff, 1982), to our knowledge there are no published examples of gap junctions between paranodal loops or between layers of myelin at Schmidt-Lanterman incisures in the PNS of any vertebrate. Likewise, there are no published reports documenting the presence of any connexin in any ultrastructurally defined gap junctions in PNS myelin. Although our LM labelling for Cx29 at presumptive incisures

was robust, immunogold labelling for Cx29 did not reveal ultrastructurally defined gap junctions at incisures or directly linking successive paranodal loops. Thus, as noted by others (Scherer *et al.*, 1995; Balice-Gordon *et al.*, 1998), it remains to be determined if gap junctions link successive myelin layers at paranodes.

In any case, the present report is the first to document Cx29 in rosettes and gap junction-like IMP arrays in the innermost layer of peripheral myelin and at the tips of paranodal loops adjacent to axon plasma membrane. In normal mice, the rosettes and IMP clusters appear identical to distinctive rosettes of P-face IMPs previously described in the innermost layer of myelin (Miller & Pinto da Silva, 1977). Miller & Pinto da Silva (1977) also found unusual rosettes of *E-face* IMPs in the axonal plasma membrane, but despite extensive searches, they were unable to detect corresponding rosettes of E-face pits in inner myelin E-faces or P-face pits in the axonal membrane and could not determine if the axonal and myelin rosettes were structurally coupled. Likewise, we did not detect Cx29 on myelin E-faces, nor did we detect Cx29 labelling of the axonal rosettes. Thus, the structural relationship of myelin rosettes with other adjacent membranes and the protein composition of the coupling partner, if any, for Cx29 are yet to be determined. Possibilities include: (i) that Cx29 in the innermost layer of myelin may not couple to another connexin (i.e. that Cx29 is present as ‘hemichannels’ that appose the axon plasma membrane); (ii) that Cx29 may couple to some other as yet unidentified neuronal connexin in the axon plasma membrane; or (iii) that Cx29 links to a non-connexin protein in the axonal plasma membrane, most likely a protein in the axonal ‘rosettes’ of E-face IMPs.

Implications for peripheral neuropathy in CMTX

In addition to the presence of Cx32 in Schwann cells, Cx32 is expressed in many tissues. Indicative of the importance of Cx32 are functional and structural impairments in peripheral nerve as well as other tissues in Cx32 knockout mice (Anzini *et al.*, 1997; Sutor *et al.*, 2000). Although CNS abnormalities possibly related to Cx32 expression in oligodendrocytes have been observed in patients with CMTX neuropathy (Bahr *et al.*, 1999), the absence of impairments in other tissues expressing mutated forms of Cx32 remains unexplained. One possibility suggested was that other connexins compensate for loss of Cx32 in some tissues, whereas the apparent expression of only Cx32 in Schwann cells may render them selectively vulnerable to mutations in this connexin (Scherer, 1996). Although the present demonstration of Cx29 in Schwann cell myelin makes this possibility less tenable, it remains to be determined whether Cx29 is able to compensate for absence of Cx32, and whether these two connexins subserve similar or different functions in peripheral nerve. Similar considerations apply regarding CMTX impairments in the CNS, as we have observed (Nagy *et al.*, 2002) localization of Cx29 at gap junctions formed by oligodendrocytes in brain.

Acknowledgements

We thank B. McLean for technical assistance and V.A. Ionescu for aid in animal preparation. We also thank Dr K. Willecke (University of Bonn, Germany) for provision of Cx32 knockout mice and Dr E.L. Hertzberg (Albert Einstein College of Medicine, New York) for providing anti-Cx32 antibodies 73F and 7C7. This work was supported by grants from the Canadian Institutes of Health Research to JIN, and by NIH grants NS31027, NS39040 and NS38121 to J.E.R.

References

Altevogt BM, Paul DL, Goodenough DA. Cloning and characterization of a novel central nervous system specific connexin, mouse connexin29. Mol Biol Cell 2000;11:1713.

Anzini P, Neuberg DHH, Schachner M, Nelles E, Willecke K, Zielasek J, Toyka KV, Suter U, Martini R. Structural abnormalities and deficient maintenance of peripheral nerve myelin in mice lacking the gap junction protein connexin32. J Neurosci 1997;17:4545–4551. [PubMed: 9169515]

Arroyo EJ, Scherer SS. On the molecular architecture of myelinated fibres. Histochem Cell Biol 2000;113:1–18. [PubMed: 10664064]

Bahr M, Andres F, Timmerman V, Nelis ME, Van Broeckhoven C, Dichgans J. Central visual, acoustic and motor pathway involvement in Charcot-Marie-Tooth family with an asn205ser mutation in the connexin32 gene. J Neurol Neurosurg Psychiatry 1999;66:202–206. [PubMed: 10071100]

Balice-Gordon RJ, Bone LJ, Scherer SS. Functional gap junctions in the Schwann cell myelin sheath. J Cell Biol 1998;142:1095–1104. [PubMed: 9722620]

Bergoffen J, Scherer SS, Wang S, Oronzi-Scott M, Bone L, Paul DL, Chen K, Lensch MW, Chance P, Fischbeck K. Connexin mutations in X-linked Charcot-Marie-Tooth disease. Science 1993;262:2039–2042. [PubMed: 8266101]

Bone LJ, Deschênes SM, Balice-Gordon RJ, Fischbeck KH, Scherer SS. Connexin 32 and X-linked Charcot-Marie-Tooth disease. Neurobiol Dis 1997;4:221–230. [PubMed: 9361298]

Challcroft JP, Bullivant S. An interpretation of liver cell membrane and junction structure based on observation of freeze-fracture replicas of both sides of the fracture. J Cell Biol 1970;47:49–60. [PubMed: 4935338]

Chandross KJ. Nerve injury and inflammatory cytokines modulate gap junctions in the peripheral nervous system. Glia 1998;24:21–31. [PubMed: 9700486]

Condorelli DF, Belluardo N, Torvato-Salinaro A, Mudo G. Expression of Cx36 in mammalian neurons. Brain Res Rev 2000;32:72–85. [PubMed: 10751658]

Ghabriel MN, Allt G. Incisures of Schmidt-Lanterman. Prog Neurobiol 1981;17:25–58. [PubMed: 7323300]

Goodenough DA, Goliger JA, Paul DL. Connexins, connexons and intercellular communication. Annu Rev Biochem 1996;65:475–502. [PubMed: 8811187]

Green ER, Harfst E, Gourdie RG, Severs NJ. Analysis of the rat liver gap junction protein: clarification of anomalies in its molecular size. Proc R Soc Lond 1988;233:165–174. [PubMed: 2898146]

Li J, Hertzberg EL, Nagy JI. Connexin32 in oligodendrocytes and association with myelinated fibers in mouse and rat brain. J Comp Neurol 1997;379:571–591. [PubMed: 9067844]

Lynn BD, Li X, Cattini PA, Turley EA, Nagy JI. Identification of sequence, protein isoforms and distribution of the hyaluronan-binding protein RHAMM in adult and developing rat brain. J Comp Neurol 2001;437:315–330. [PubMed: 11596057]

Mambetisaeva ET, Gire V, Evans WH. Multiple connexin expression in peripheral nerve, Schwann cells, and Schwannoma cells. J Neurosci Res 1999;57:166–175. [PubMed: 10398294]

Matesic DF, Germak JA, Dupont E, Madhukar BV. Immortalized hypothalamic luteinizing hormone-releasing hormone neurons express a connexin26-like protein and display functional gap junction coupling assayed by fluorescence recovery after photobleaching. Neuroendocrinology 1993;58:485–492. [PubMed: 8115017]

Miller RG, Pinto Da Silva P. Particle rosettes in the periaxonal Schwann cell membrane and particle clusters in the axonlemma of rat sciatic nerve. Brain Res 1977;130:135–141. [PubMed: 884515]

Nagy JI, Dudek FE, Rash JE. Update on connexins and gap junctions in neurons and glia in the mammalian nervous system. Brain Res Rev. 2002in press

Nagy JI, Li X, Rempel J, Stelmack G, Patel D, Staines WA, Yasumura T, Rash JE. Connexin26 in adult rodent central nervous system: demonstration at astrocytic gap junctions and colocalization with connexin30 and connexin43. J Comp Neurol 2001;441:302–323. [PubMed: 11745652]

Nagy JI, Rash JE. Connexins and gap junctions of astrocytes and oligodendrocytes in the CNS. Brain Res Rev 2000;32:29–44. [PubMed: 10751655]

Rash JE, Staines WA, Yasumura T, Patel D, Hudson CS, Stelmack GL, Nagy JI. Immunogold evidence that neuronal gap junctions in adult rat brain and spinal cord contain connexin36 but not Cx32 or Cx43. Proc Nat Acad Sci USA 2000;97:7573–7578. [PubMed: 10861019]

Rash JE, Yasumura T. Direct immunogold labeling of connexins and aquaporin4 in freeze-fracture replicas of liver, brain and spinal cord: factors limiting quantitative analysis. Cell Tissue Res 1999;296:307–321. [PubMed: 10382274]

Rash JE, Yasumura T, Dudek FE, Nagy JI. Oligodendrocytes form intercellular gap junctions exclusively with astrocytes: Demonstration by light microscopic immunocytochemistry and freeze-fracture replica immunogold labeling (FRIL). J Neurosci 2001;21:1983–2000. [PubMed: 11245683]

Sahenk Z, Chen L. Abnormalities in the axonal cytoskeleton induced by a connexin32 mutation in nerve xenografts. J Neurosci Res 1998;51:174–184. [PubMed: 9469571]

Sandri C, Van Buren JM, Akert K. Membrane morphology of the vertebrate nervous system: a study with freeze-etch technique. Prog Brain Res 1977;46:1–384. [PubMed: 854571]

Scherer SS. Molecular specializations at nodes and paranodes in peripheral nerve. Microsc Res Techn 1996;34:452–461.

Scherer SS, Deschenes SM, Xu YT, Grinspan JB, Fischbeck KH, Paul DL. Connexin32 is a myelin-related protein in the PNS and CNS. J Neurosci 1995;15:8281–8294. [PubMed: 8613761]

Severs NJ. Cardiovascular disease. Novartis Found Symp 1999;219:188–206. [PubMed: 10207905]

Simon AM, Goodenough DA. Diverse functions of vertebrate gap junctions. Trends Cell Biol 1988;8:477–483. [PubMed: 9861669]

Sohl G, Eiberger J, Jung YT, Kozak CA, Willecke K. The mouse gap junction gene connexin29 is highly expressed in sciatic nerve and regulated during brain development. Biol Chem 2001;382:973–978. [PubMed: 11501764]

Spray DC, Dermietzel R. X-linked dominant Charcot-Marie-Tooth disease and other potential gap junction diseases of the nervous system. Trends Neurosci 1995;18:256–262. [PubMed: 7570999]

Steere RL. High resolution stereography of complementary freeze-fracture replicas reveals the presence of depressions opposite membrane associated particles of split membranes. Proc Micros Soc Am 1971;29:256–262.

Suter U. Biology and genetices of hereditary motor and sensory neuropathies. Annu Rev Neurosci 1995;18:45–75. [PubMed: 7605070]

Sutor B, Schmolke C, Teubner B, Schirmer C, Willecke K. Myelination defects and neuronal hyperexcitability in the neocortex of connexin32-deficient mice. Cereb Cortex 2000;10:684–697. [PubMed: 10906315]

Tetzlaff W. Tight junction contact events and temporarygap junctions in the sciatic nerve fibres of the chicken during Wallerian degeneration and subsequent regeneration. J Neurocytol 1982;11:839–858. [PubMed: 7143029]

Trapp BD, Andrews SB, Cootauco C, Quarles R. The myelin-associated glycoprotein is enriched in multivesicular bodies and periaxonal membranes of actively myelinating oligodendrocytes. J Cell Biol 1989;109:2417–2426. [PubMed: 2478568]

Veenstra RD. Size and selectivity of gap junction channels formed from different connexins. J Bioenerg Biomem 1996;28:327–337.

White TW, Bruzzone R. Multiple connexin proteins in single intercellular channels: connexin compatibility and functional consequences. J Bioenerg Biomem 1996;28:339–350.

Willecke K, Eiberger J, Degen J, Eckardt D, Romualdi A, Guldenagel M, Deutsch U, Sohl G. Structural and functional diversity of connexin genes in the mouse and human genome. Biol Chem 2002;383:725–737. [PubMed: 12108537]

Yoshimura T, Satake M, Kobayashi T. Connexin43 is another gap junction protein in the peripheral nervous system. J Neurochem 1996;67:1252–1258. [PubMed: 8752133]

Zhao, S.; Spray, DC. Localization of Cx26, Cx32 and Cx43 in myelinating Schwann cells of mouse sciatic nerve during postnatal development. In: Werner, R., editor. Gap Junctions. IOS Press; Amsterdam: 1998. p. 198-202.

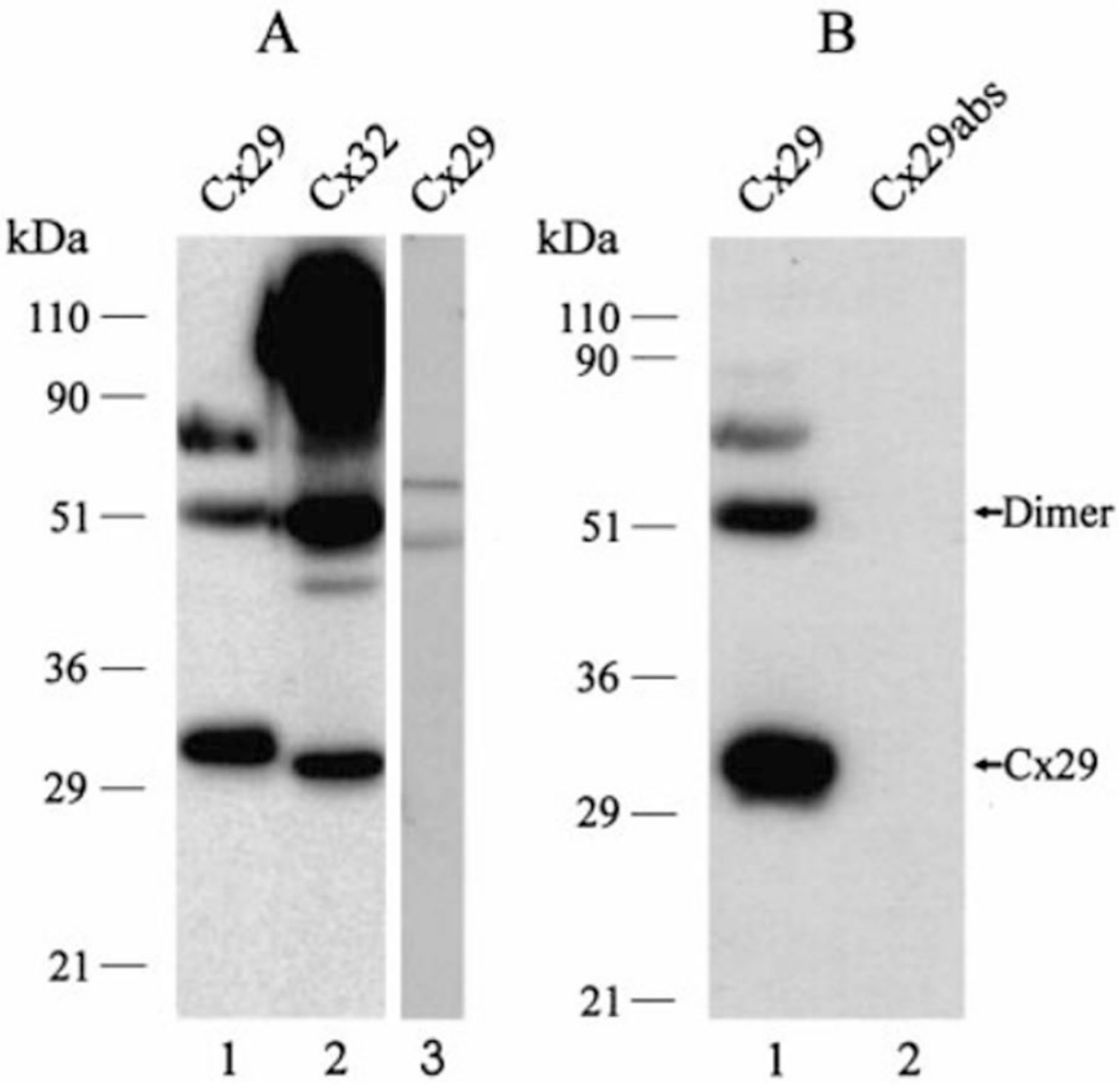

Fig. 1.

Western blots of Cx29 in sciatic nerve and Cx32 in liver. (A) Sciatic nerve homogenate probed with anti-Cx29 (lane 1) and, shown for comparison, liver homogenate probed with anti-Cx32 (antibody 73F, lane 2) and with anti-Cx29 (lane 3). Monomer and putative higher molecular weight forms of Cx29 are detected in nerve, and multiple forms of Cx32 are detected in liver. Cx29 migrates slightly slower than Cx32, and anti-Cx29 does not react with Cx32 in liver. (B) Sciatic nerve homogenate probed with anti-Cx29 (lane 1), and with anti-Cx29 after preadsorption with immunizing peptide (lane 2) showing elimination of all bands.

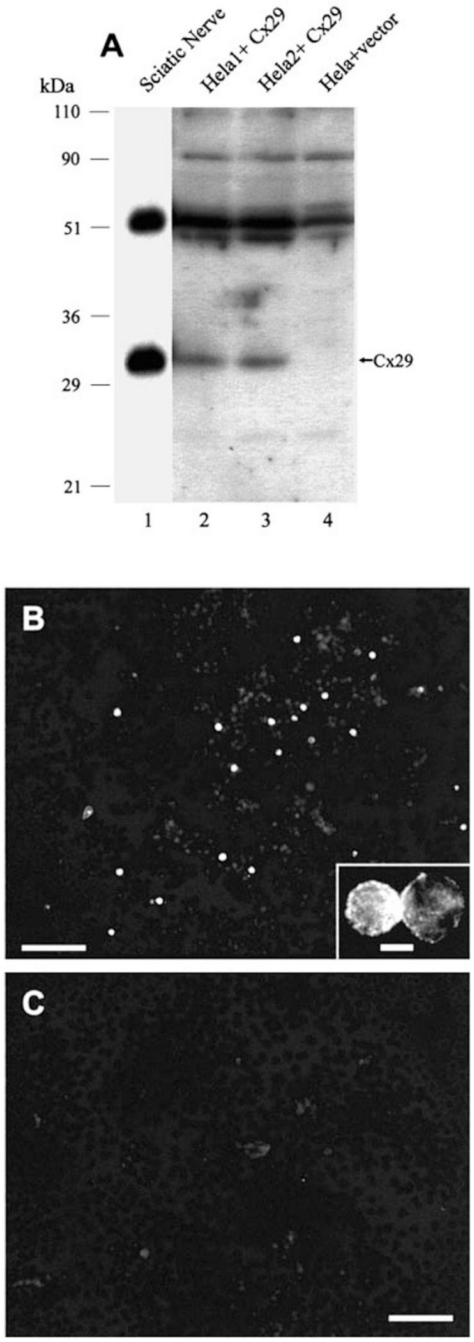

Fig. 2.

(A) Western blots of Cx29 in HeLa cells transiently transfected with Cx29 cDNA. Lysates from two separate cultures of cells transfected with Cx29 expression vector show antibody detection of monomeric Cx29 (lanes 2 and 3) corresponding to that of Cx29 in homogenate of sciatic nerve (lane 1), while no detection is seen in control HeLa cells transfected with empty vector (lane 4). (B and C) Immunofluorescence of Cx29 in transfected HeLa cells showing robust immunolabelling in a small percentage of cells (B), and total absence of labelling in cells transfected with empty vector (C). Inset shows immunofluorescence within a pair of cells and around their periphery. Scale bar, 100 μm (B and C), 25 μm (inset).

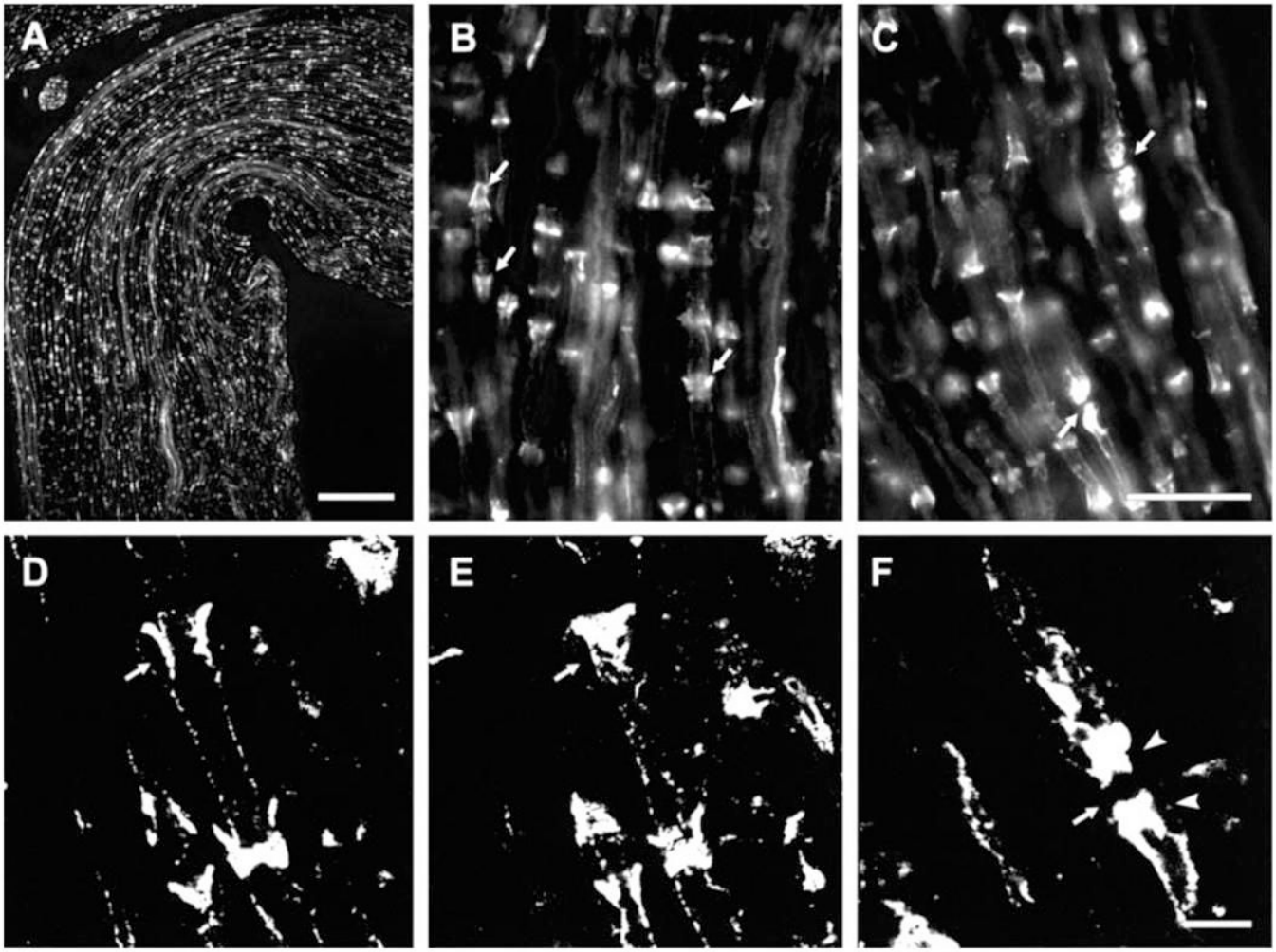

Fig. 3.

Immunofluorescence of Cx29 in sections of sciatic nerve from CD1 mice. (A) Low magnification showing distribution of labelling with anti-Cx29 antibody. (B and C) Magnifications showing labelling of either conical structures (B, arrows) or bands (B, arrowhead) orientated perpendicular to the long axis of fibers, and accumulation of staining at nodes of Ranvier (C, arrows). (D and E) Laser scanning confocal micrographs of the same field at different planes of focus showing collar of immunolabelling midway through a fibre (D, arrow) and closer to its surface (E, arrow). Note absence of labelling within the axon in D. (F) Confocal micrograph showing accumulation of labelling for Cx29 on each side (arrowheads) of a node of Ranvier (arrow). Scale bars, 100 μm (A); 25 μm (B and C); 5 μm (D–F).

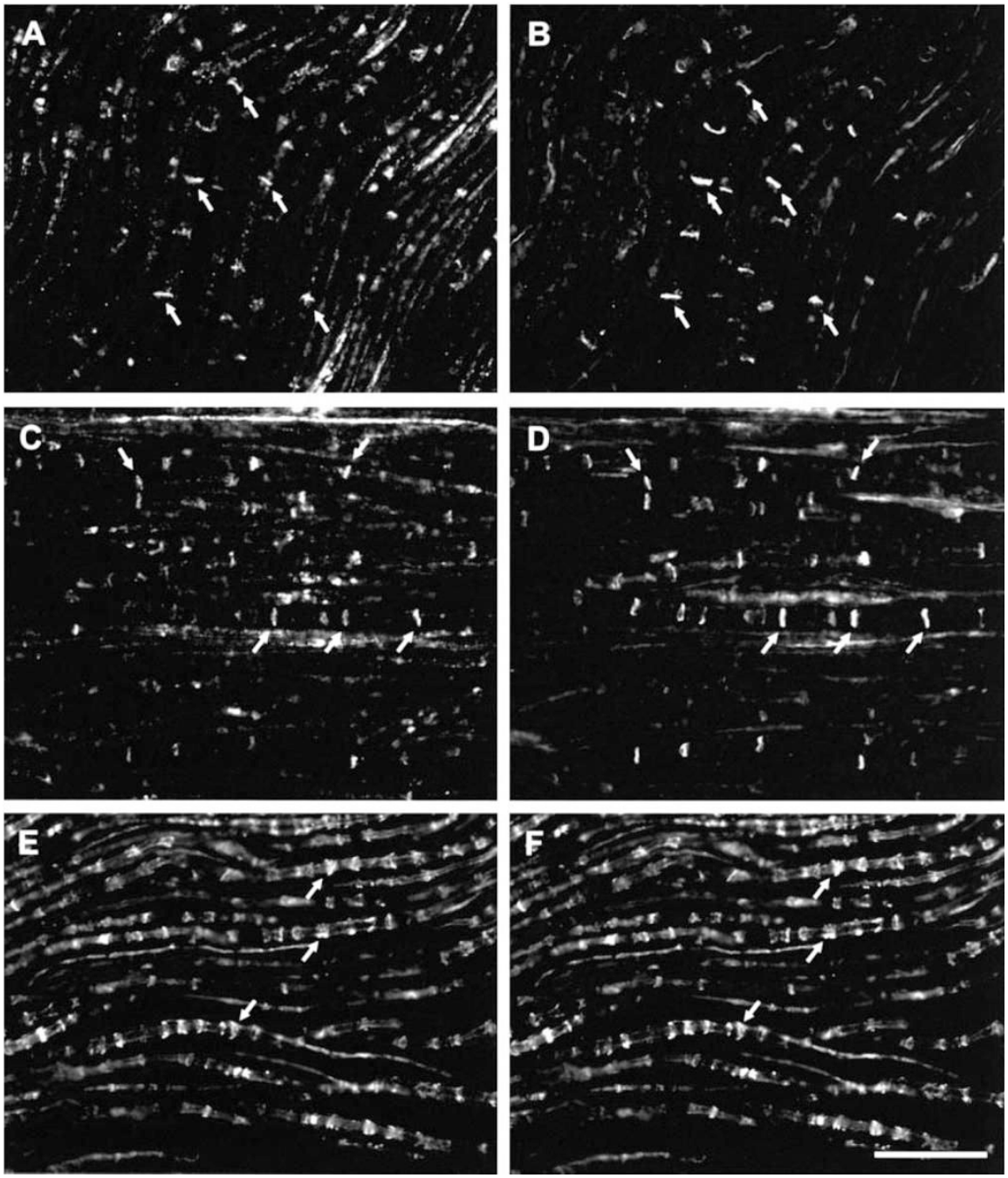

Fig. 4.

Double immunofluorescence labelling of Cx29 with Cx32 and MAG in mouse sciatic nerve. (A and B) Same field of a section showing labelling with anti-Cx29 (A) and labelling for Cx32 with monoclonal antibody 73F (B). (C and D) Same field of a section showing labelling with anti-Cx29 (C) and labelling for Cx32 with monoclonal antibody 7C7. (E and F) Same field of a section showing labelling with anti-Cx29 (E) and with anti-MAG (F). Corresponding arrows in (A and B), (C and D) and (E and F) indicate double-labelled structures. Scale bars, 50 μm.

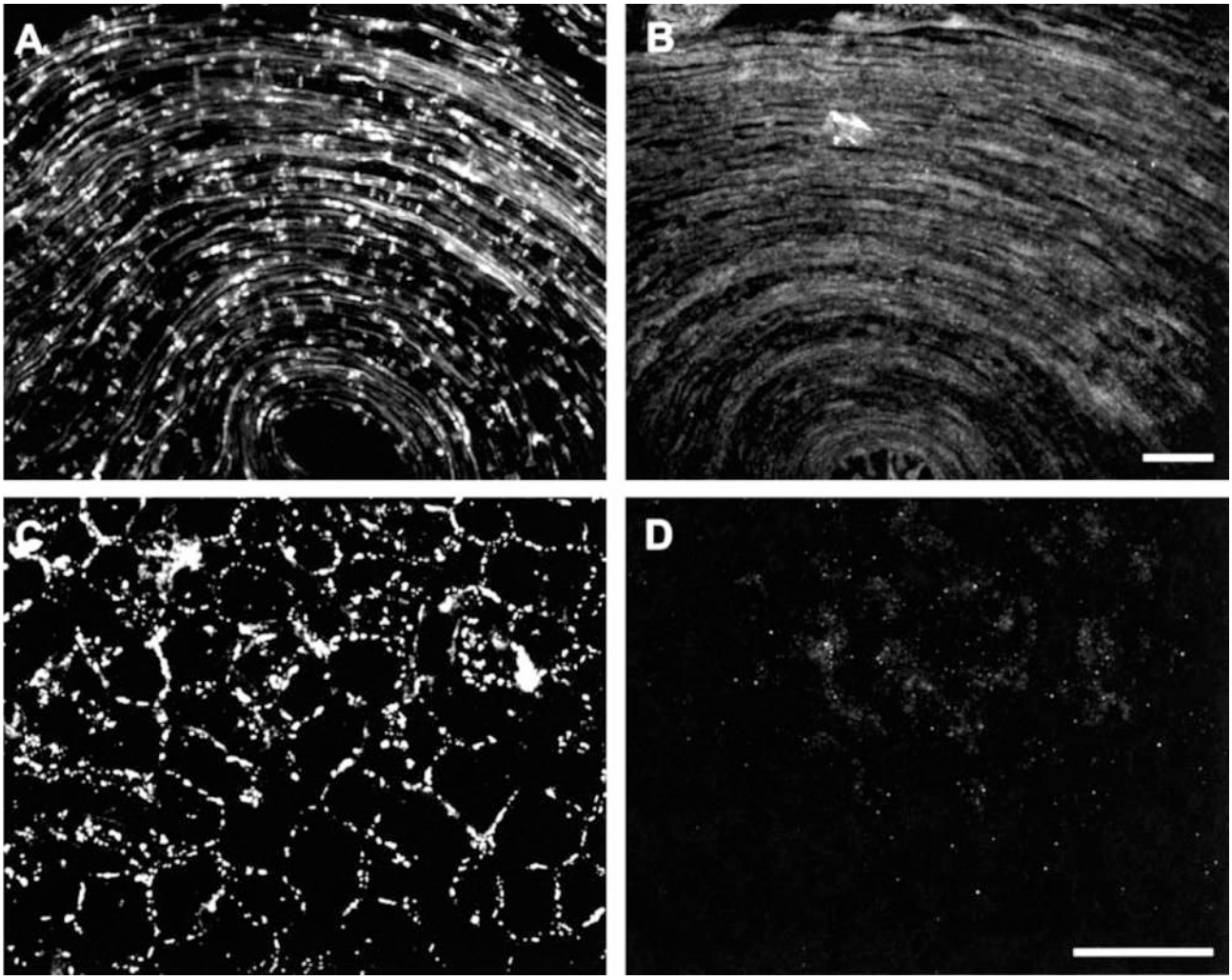

Fig. 5.

Specificity of immunofluorescence labelling of Cx29. (A) Field in a section of sciatic nerve processed with anti-Cx29 antibody, and (B) the same field in an adjacent section showing elimination of labelling after preadsorption of anti-Cx29 with immunizing peptide. The field shown is the apex of a hairpin loop in the section, resulting in curvature of fibers. (C and D) The same field in a section of liver processed for immunofluorescence with anti-Cx32 and anti-Cx29 antibody. Punctate labelling occurs around hepatocytes with anti-Cx32 7C7 (A) and no labelling is present with anti-Cx29 (B), indicating lack of cross reaction of the latter with Cx32. Scale bar, 50 μm.

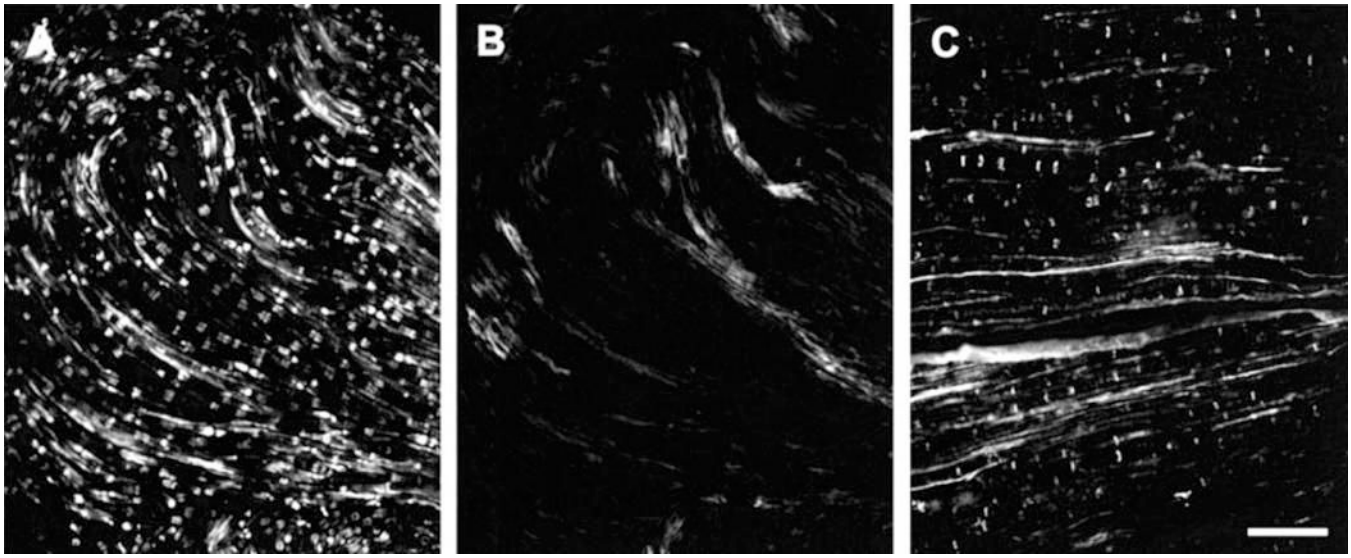

Fig. 6.

Double immunofluorescence for Cx29 and Cx32 in sciatic nerve of Cx32 knockout mice (strain C57BL/6). (A and B) The same field in a section from Cx32 knockout mouse processed with anti-Cx29 antibody (A) and monoclonal anti-Cx32 (B) antibody 73F. (C) Normal labelling for Cx32 in sciatic nerve of wild-type mouse strain C57BL/6. Absence of labelling in section devoid of Cx32 (B) indicates lack of cross-reaction of anti-Cx32 antibody with Cx29. Scale bars, 50 μm.

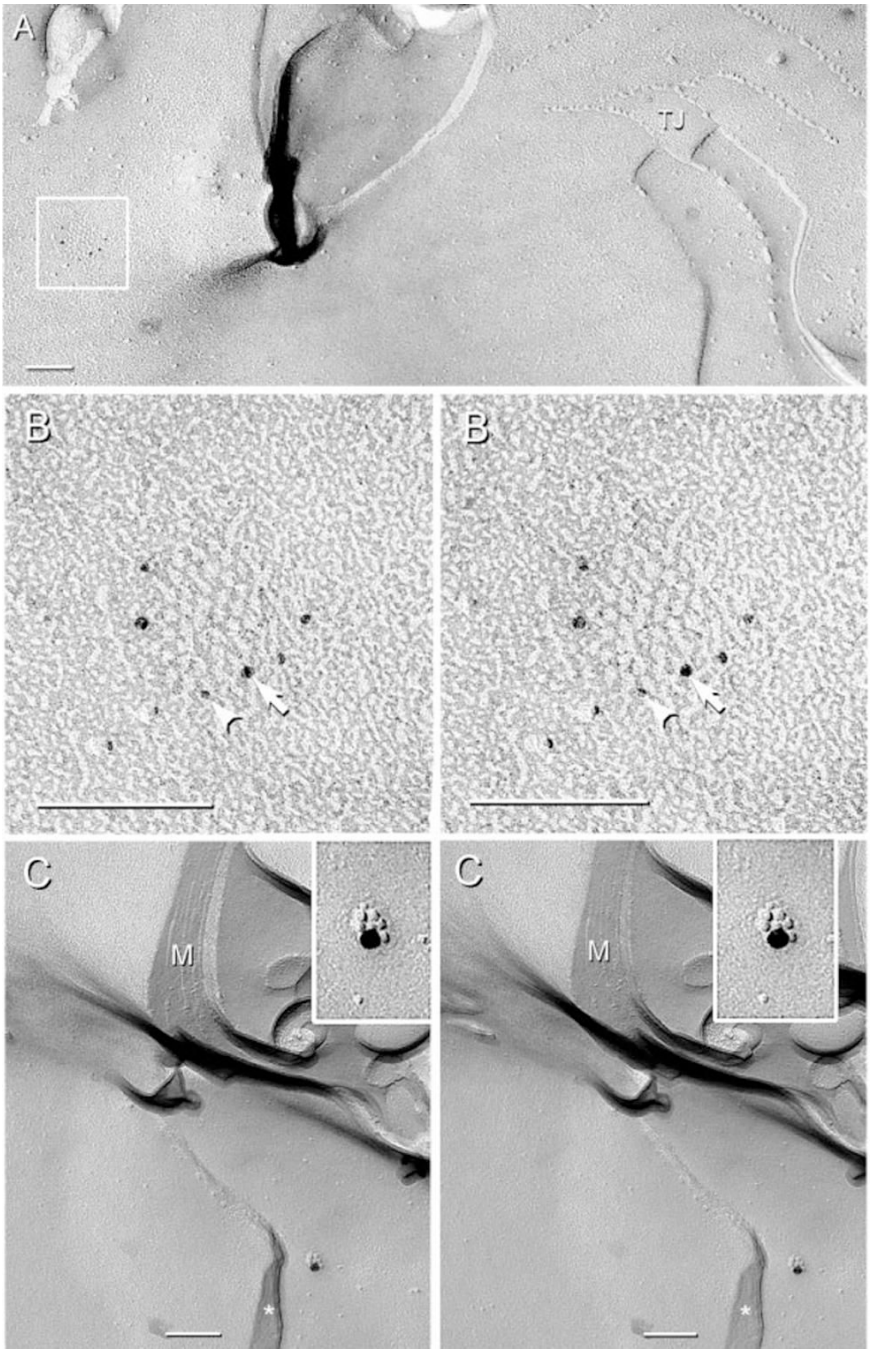

Fig. 7.

FRIL images of gap junctions labelled for Cx32 in normal adult mouse sciatic nerve. (A) Gap junction between outer tongue and second layer of myelin (M) (boxed area). A multistranded tight junction (TJ) also links the outer tongue E-face with the P-face of second myelin layer. (B) Magnification of the boxed gap junction in A. The E-face of the junction is visualized, with connexins of the underlying hemiplaque labelled for Cx32 by four 5-nm gold beads (arrowhead) and two 6-nm gold beads (arrow). In this reverse ('intaglio') stereoscopic image, gold beads appear on top of the inverted replica for easier visualization. (C) P-face of the second outermost layer of myelin showing a gap junction composed of seven connexon IMPs labelled

for Cx32 by a single 18-nm gold bead. Cytoplasm within the outer tongue of myelin is indicated by an asterisk. Scale bars, 0.1 μm.

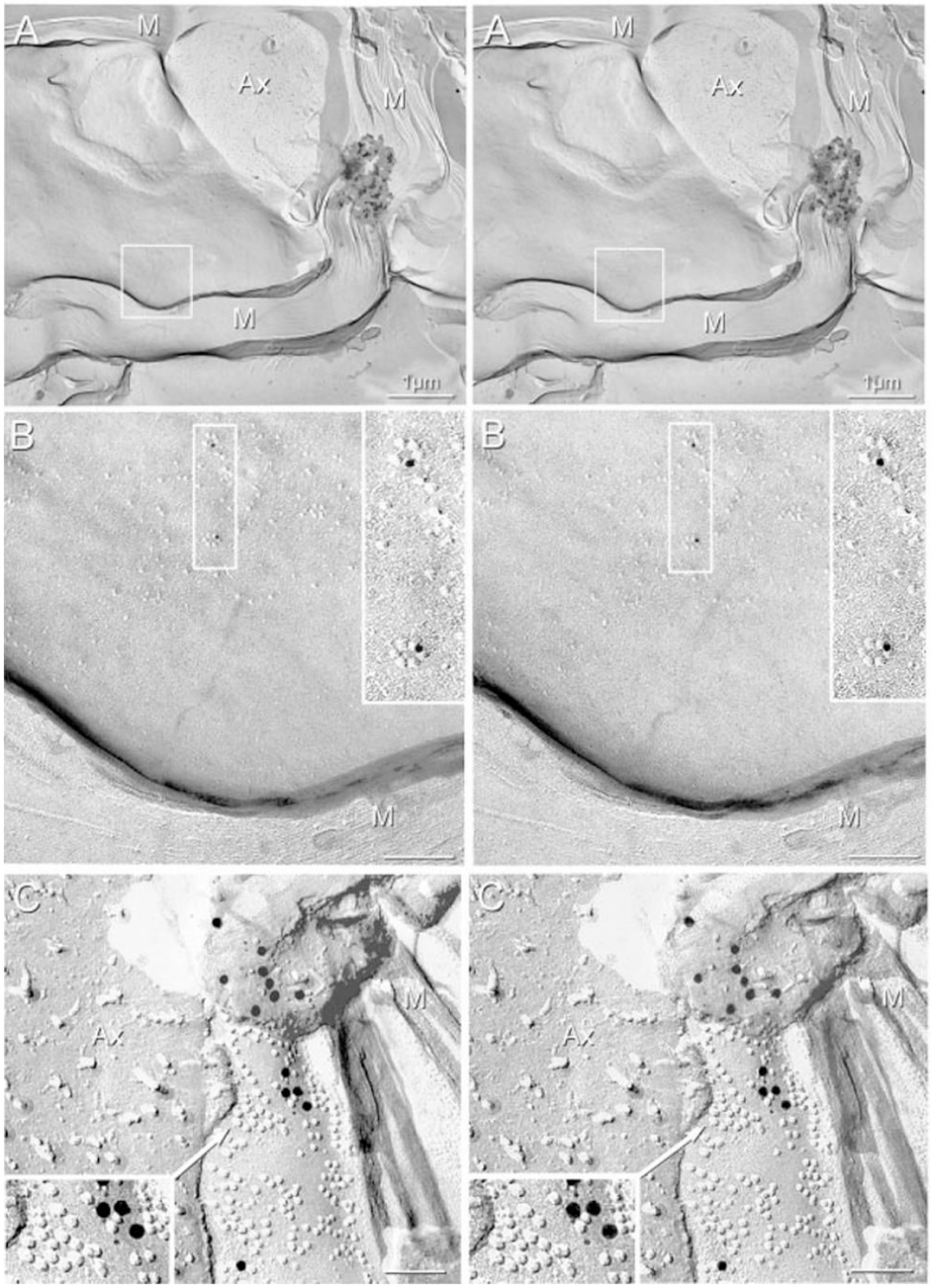

Fig. 8.

Stereoscopic images of P-face IMPs in the innermost myelin layer (M) of sciatic nerve after double-labelling for Cx32 and Cx29. (A and B) Normal sciatic nerve showing two IMP rosettes (boxed area in A, magnified in B and further magnified in B, inset). Each rosette is labelled for Cx29 (12-nm gold). (C) Sciatic nerve from Cx32 KO mouse. IMPs in rosettes and clusters are immunogold labelled for Cx29, with both 6- and 18-nm gold beads present beneath P-face IMPs. Labeling extends beneath the replicated, partially dislodged fragment. Magnified image in inset shows interlocking IMP rosettes in association with clusters of similar 8-nm IMPs labelled with four 6-nm and four 18-nm gold beads. No labelling for Cx32 (12-nm gold) was

detected beneath rosettes or IMP clusters in innermost myelin layers of normal or Cx32 KO mice. Ax, Axon; M, cross-fractured myelin. Scale bars, 0.1 μm.

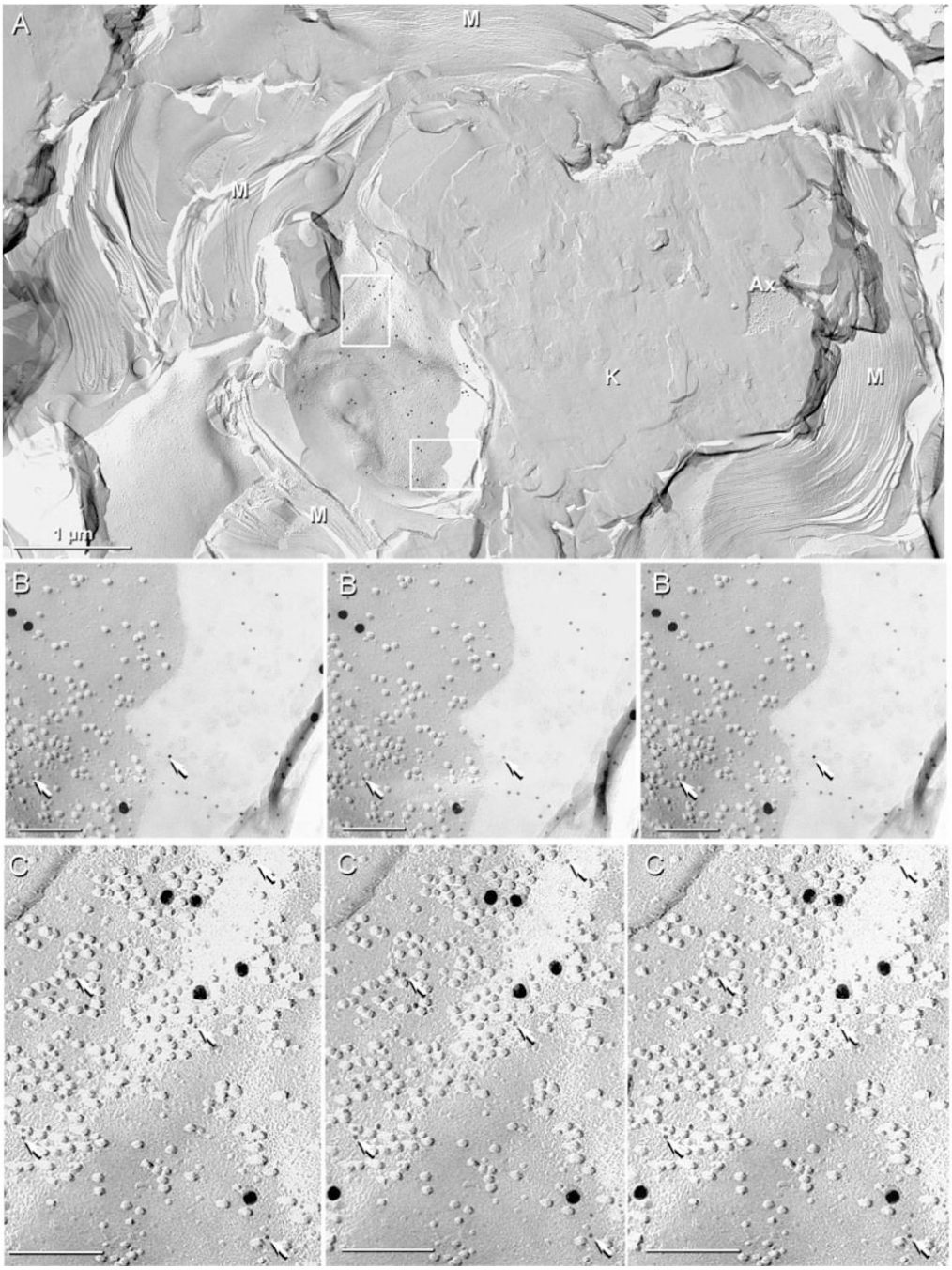

Fig. 9.

IMP rosettes and clusters in innermost myelin layer in sciatic nerve of Cx32 KO mouse after double-labelling for Cx29 (6 and 18-nm gold) and Cx32 (12-nm gold; none present). Label for Cx29 is abundant beneath P-face IMPs in the innermost layer of myelin (A, inscribed boxes), but was absent in other layers of myelin (A, lower left) or in areas of knife scrape (K) (A, centre-right). (B) Magnification of lower box in A. The 6-nm gold beads (arrows) are more easily seen in areas where shadowed debris prevented platinum deposition. In the area not coated with platinum, IMPs are faintly delineated by the very thin, rotary-deposited carbon film. (C) Magnified upper box in A showing clustered IMPs labelled with six 18-nm and 24 6-nm gold beads (arrows). The 6-nm gold beads are more readily evident by first viewing the

intaglio images (right two images), then the true stereoscopic perspective (left two images). Scale bars, 1 μm (A); 0.1 μm (B and C).